Published in final edited form as:
Angew Chem Int Ed Engl. 2014 July 14; 53(29): 7574–7578. doi:10.1002/anie.201402472.

Iron Porphyrin Carbene Catalytic Intermediates: Structures, Mössbauer and NMR Spectroscopic Properties, and Bonding**

Rahul L. Khade,
Department of Chemistry, Chemical Biology, and Biomedical Engineering, Stevens Institute of Technology, Castle Point on Hudson, Hoboken NJ 07030 (USA), Fax: (+) 1-201-216-8240

Wenchao Fan,
Department of Chemistry, Chemical Biology, and Biomedical Engineering, Stevens Institute of Technology, Castle Point on Hudson, Hoboken NJ 07030 (USA), Fax: (+) 1-201-216-8240

Dr. Yan Ling,
Department of Chemistry and Biochemistry, University of Southern Mississippi, 118 College Drive #5043, Hattiesburg, MS 39406 (USA)

Liu Yang,
Department of Chemistry, Chemical Biology, and Biomedical Engineering, Stevens Institute of Technology, Castle Point on Hudson, Hoboken NJ 07030 (USA), Fax: (+) 1-201-216-8240

Prof. Dr. Eric Oldfield, and
Department of Chemistry, University of Illinois at Urbana-Champaign, 600 South Matthews Avenue, Urbana, IL 61801 (USA)

Prof. Dr. Yong Zhang
Department of Chemistry, Chemical Biology, and Biomedical Engineering, Stevens Institute of Technology, Castle Point on Hudson, Hoboken NJ 07030 (USA), Fax: (+) 1-201-216-8240

Yong Zhang: yong.zhang@stevens.edu

Abstract

Iron porphyrin carbenes (IPCs) are thought to be intermediates involved in the metabolism of various xenobiotics by cytochrome P450, as well as in chemical reactions catalyzed by metalloporphyrins and engineered P450s. While early work proposed IPCs to contain Fe^{II}, more recent work invokes a double bond description of the iron carbon bond, similar to that found in Fe^{IV} porphyrin oxenes. Here, we report the first quantum chemical investigation of IPC Mössbauer and NMR spectroscopic properties, as well as their electronic structures, together with comparisons to ferrous heme proteins and an Fe^{IV} oxene model. The results provide the first accurate predictions of the experimental spectroscopic observables as well as the first theoretical explanation of their electrophilic nature, as deduced from experiment. The preferred resonance structure is $Fe^{II}\leftarrow\{:C(X)Y\}^0$ and not $Fe^{IV}=\{C(X)Y\}^{2-}$, a result that will facilitate research on IPC reactivities in various chemical and biochemical systems.

**This work was supported by NSF grant CHE-1300912 to YZ and NIH grants GM085774 toYZ and GM065307 to EO.

Correspondence to: Yong Zhang, yong.zhang@stevens.edu.

Supporting information for this article is available on the WWW under http://www.angewandte.org.

Keywords

carbenes; catalysts; porphyrins; metalloenzymes; quantum chemistry

P450 cytochromes are a ubiquitous family of heme proteins that act as catalysts for numerous biochemical reactions with high valent ferryl species having been found to be important catalytic intermediates.[1] Biomimetic P450 metalloporphyrin models have also been found to be efficient catalysts for a broad range of organic reactions including C-H insertion, N-H insertion, cyclopropanation, as well as the olefination of aldehydes and ketones.[2] The active species responsible for such reactivities have been proposed to be metalloporphyrin carbene complexes. In particular, iron porphyrin carbene (IPC) complexes have been shown to undergo several of these reactions, including C-H insertions and cyclopropanations.[2f] IPC complexes were first observed several decades ago in the reactions of polyhalogenated methanes with porphyrins,[3] reactions similar to those observed in the metabolism by cytochrome P450 of various xenobiotics, including toxic polyhalogenated compounds as well as diverse drugs.[4] More recently, engineered cytochrome P450s have been used in synthetically important reactions not observed in nature,[2a] carbene transfers, with IPC complexes again being thought to be key catalytic intermediates.

Given the broad general interest in IPCs in chemistry and biochemistry, it is surprising that the electronic structures and associated reactivities of IPC complexes are poorly understood. For instance, whether IPCs are best described as $Fe^{II}\leftarrow\{:C(X)Y\}^0$ or $Fe^{IV}=\{C(X)Y\}^{2-}$ (similar to $Fe^{IV}=O^{2-}$ in conventional P450 reactions), has not been resolved.[2f, 5] The presence of Fe^{II} was first proposed based on similarities with the UV-vis and NMR spectra of diamagnetic Fe^{II} porphyrins,[5c, d] and also used in an early extended Hückel theory study,[6] while in later work the presence of Fe^{IV} was proposed, based on similarities with the Mössbauer spectra of Fe^{IV} proteins and model systems.[2f, 5e] The double bond feature of the iron carbene bond in IPCs now seems generally accepted in the catalysis and biocatalysis areas,[2a-c, 2f, 2h, 5a] but has not, however, been investigated by *ab initio* quantum chemical methods. In addition, although IPCs were reported to effect electrophilic reactions via positive charge build-up on the substrates (Scheme 1),[2f, 2h, 5a, 7] there are no theoretical studies that explain this catalytic reactivity. Here, we use density functional theory (DFT) calculations to provide the first predictions of the Mössbauer and NMR spectroscopic observables of IPC complexes, as well as their geometries, and on the basis of these results together with a detailed investigation of molecular orbitals and charges, we determined the origins of their reactivity. In particular, the preferred resonance structure was found to be quite different to that currently used in experimental studies of IPCs.

We initially calculated the Mössbauer spectra of IPCs since the ability to predict spectroscopic observables can reasonably be expected to give some confidence in the quality of the calculations and hence, confidence in other computed properties. We first used X-ray structures[2f, 5c] to compute the Mössbauer spectra of "typical" Fe^{IV} and Fe^{II} complexes, **1** and **2**, Figure 1. **1** contains an Fe=O bond and is the first Fe^{IV} complex with a reported X-ray structure,[8] while the heme site in carbomonoxymyogolobin (MbCO) is known to

possess an Fe^{II} center.[9] We used the density functional theory (DFT) methods described previously. These enabled excellent predictions of the Mössbauer isomer shift (δ_{Fe}) and quadrupole splitting (ΔE_Q) values in >50 iron proteins and model systems encompassing the most common iron spin (S = 0, ½, 1, 3/2, 2, 5/2), oxidation (Fe^0, Fe^{II}, Fe^{III}, Fe^{IV}, Fe^{VI}), and coordination (2,3,4,5,6) states,[10] see Supporting Information for computational details of the methods used here.

We first calculated the Mössbauer properties of **1** and **2** with all possible spin states and also evaluated the relative stability of other spin states with respect to the singlet state ($\Delta E_{S=0}$). As shown in Table 1, the calculations correctly reproduced the experimental ground states of a triplet for **1** and a singlet for **2**,[8, 9b] and only computed results obtained by using experimental spin states produced good predictions of both Mössbauer parameters, giving confidence in the methods used. We then investigated IPCs **3–5**, Figure 1, intermediates in catalysis and the degradation of polyhalogenated compounds. All porphyrin *meso*-substituents were replaced with hydrogens to facilitate calculations. **3** is the only known IPC characterized by both X-ray crystallography and Mössbauer spectroscopy and the DFT results again reproduced the known singlet ground state, as well as providing good agreement between both of the experimental Mössbauer parameters and theory (Table 1). The predicted $\delta_{Fe}/\Delta E_Q$ values of 0.19/−1.76 mm/s in **4** and 0.061/−1.94 mm/s in **5** were similar to those obtained with **3**. So, overall, the Mössbauer isomer shifts in these IPC complexes are similar to the experimental results of ~0.09–0.22 mm/s in non-porphyrin iron carbene complexes.[11]

In contrast to the rather small range of δ_{Fe} values in IPCs, ΔE_Q values cover a larger range since ΔE_Q is related to the electric field gradient (EFG) tensor at the nucleus, which is more sensitive to the molecular environment than is δ_{Fe}.[9b, 10d, 11] For instance, compared to the five-coordinate system **3**, the six-coordinate complex **4** has a smaller absolute ΔE_Q value, due to increased symmetry and thus, a reduced EFG. It is of interest to note that the δ_{Fe} values in the IPCs are close to the experimental results of ~0.03–0.17 mm/s for Fe^{IV} species,[5e, 12] which was previously used to support the presence of an Fe^{IV} feature in IPCs[2f, 5e] since in general, δ_{Fe} is a good indicator of iron oxidation state.[9b, 10c] However, exceptions were found due to strong ligand interactions,[13] and some non-porphyrin iron carbenes have been reported to be Fe^{II} systems.[11]

In contrast to δ_{Fe} results (which show similarities to Fe^{IV} systems), the relative stability of the spin states for the five-coordinate IPC complex **3** are the same as the typical Fe^{II} complex, **2**, and are quite different to those found in the typical Fe^{IV} complex **1**, Table 1. The six-coordinate IPC complex **4** also exhibits the same trend with $\Delta E_{s=0}$ for the S=1 state being 17.70 kcal/mol higher, and for the S=2 state, 41.18 kcal/mol higher, indicating, again, similarities to Fe^{II} complexes.

To further investigate the Fe^{II}/Fe^{IV} bonding puzzle, we investigated the geometry optimized structures of IPCs. Since there are no prior reports of this kind of study, we evaluated a number of DFT methods including the commonly used hybrid functional B3LYP and another hybrid functional, mPW1PW91, as well as the more recently developed functionals M06, B97D, and ωB97XD, together with several basis sets (see Supporting Information for

details). The key geometric parameters of interest are those around the carbene center: the iron carbene bond length R_{FeC}, the average iron and porphyrin-nitrogen bond length R_{FeN}, and the average length between the carbene carbon and its attached carbons, R_{CC}. The best predictions are shown in Table 2 and have only a 0.012 Å mean absolute deviation (0.65% mean percentage deviation) for the singlet ground state. In contrast, results from using higher spin states (S=1 and 2) have significantly larger errors, with 0.069 and 0.133 Å mean absolute deviations, respectively. These data further support the energy results discussed above, and are consistent with the experimental NMR assignment of a diamagnetic ground state.[2f, 5c, d]

We next investigated the ^{13}C NMR shifts/shieldings in a series of IPCs in detail. As shown in Table 3, experimental solution ^{13}C NMR chemical shifts of carbene carbons encompass a broad range, from 210 to 385 ppm downfield from TMS,[2c, 2f, 5d] which suggests that these NMR shifts may serve as sensitive probes of electronic structure. We used the geometry-optimized structures together with a series of DFT functionals and basis sets as well as the incorporation of solvent effects in the NMR chemical shielding calculations (see Supporting Information for computational details). The best results are shown in Table 3. As shown in Figure 2A, there is an excellent linear correlation between theory (σ^{calc}) and experiment (δ^{expt}) for the singlet state, with the correlation coefficient R^2=0.982. The predicted shifts using this regression line (δ^{pred}'s) yielded a 6.71 ppm mean absolute deviation (2.34% mean percentage deviation), indicating that the broad range of ^{13}C NMR chemical shifts in IPCs is well reproduced in our quantum chemical calculations. In contrast, results from using S=1 or S=2 states yielded ~9000 and ~30000 ppm mean absolute deviations, respectively, due to large hyperfine shifts, Table 3. These results provide strong additional evidence for a diamagnetic ground state in these IPC complexes, quite different to the paramagnetic states seen in Fe^{IV} species in heme/non-heme proteins and model systems. [1, 8, 14] In addition, there were essentially no differences between the theory-experiment correlations when solvent effects were included (R^2 = 0.980) using the polarizable continuum method, see Table S6.

Given the success in predicting the spectroscopic observables, we next investigated the atomic charges of the carbene carbons in the IPC systems. As shown in Table 3, these charges (Q_C's) cover a large range, ~0.3 *e*. The charges are all positive, with the charges in the known catalysts **3**, **4**, and **11** being particularly large, suggesting a physical basis for their electrophilic reactivity, as proposed experimentally (Scheme 1).[2f, 2h, 5a, 7] A good correlation between these charges and the experimental NMR chemical shifts was also found, as illustrated in Figure 2B (R^2=0.958), suggesting that ^{13}C NMR spectroscopy may be used as a probe of the reactivities of other IPC complexes.

The positive charges also suggest that the dominant feature in the metal-carbene bond involves carbene-to-metal donation. That is, carbenes with more electron-withdrawing substituents (e.g. CCl_2 as opposed to CPh_2) are associated with less positive charge (see Table 3), because electron-withdrawing substituents hinder the carbene's electron donation ability. These results thus support the importance of a $Fe^{II}\leftarrow\{:C(X)Y\}^0$ resonance structure over $Fe^{IV}=\{C(X)Y\}^{2-}$ since the latter is associated with dominant metal-to-carbene back-

donation, and thus partial negative charges on the carbene carbon, inconsistent with the electrophilic reactivities seen experimentally.

To further investigate the electronic structures of IPCs we examined the molecular orbitals (MOs) of the three IPC complexes having reported X-ray structures (**3**–**5**) and compared the MO results obtained with those of typical Fe^{IV} and Fe^{II} systems (**1,2**). Although the IPCs have different structural features (five-coordinate, six-coordinate, as well as a vinylidene carbene), the electronic configurations of the frontier metal orbitals (FMOs) are the same: $(d_{xy})^2(d_{xz})^2(d_{yz})^2(dz^2)^0(dx^2–y^2)^0$, as illustrated for **3** in the left-hand column of Figure 3. This is consistent with a d^6 Fe^{II} configuration, basically as found in the typical low spin Fe^{II} system **2** reported previously[10c] and other non-catalyst IPC models.[6] In contrast, as seen in the right-hand column in Figure 3 for the typical Fe^{IV} system **1** (in the S=0 state, to be more readily compared with the diamagnetic IPCs), the FMOs are $(dxy)^2(dxz)^2(dyz)^0(dx^2–y^2)^0(dz^2)^0$, consistent with the expected d^4 Fe^{IV} configuration. This has the same energy order as the FMOs in the triplet ground state: $(dxy)^2(dxz)^1(dyz)^1(dx^2–y^2)^0(dz^2)^0$ reported previously,[15] and is clearly different to that seen in the IPC complexes. It is also interesting to note that compared to the two Fe dπ and O pπ interactions in the ground state of the Fe^{IV} complex **1**,[15] there is only one Fe dπ and C pπ interaction in the ground state of IPC complex **3**, as shown in Figure 3. The overlap-weighted natural atomic orbital bond order for Fe-O in **1**, 0.797, is ca. 50% larger than that for Fe-C in **3**, 0.548, which is further evidence for the difference between Fe-O bonding in the Fe^{IV} system and Fe-C bonding in the IPCs.

To further evaluate the possibility of the Fe^{IV} state in IPC complexes, calculations of **3** with a deliberate initial setup of Fe^{IV} and $(CPh_2)^{2-}$ and even with a different occupied Fe 3d orbital sequence (dxy > dxz/dyz) were performed. After convergence all systems yielded the same results as shown in Figure 3, additional evidence that the Fe^{IV} state is not stable in these IPC complexes.

So, the MO results together with the charges, spin state trends and NMR shifts described above are all very similar to those found in Fe^{II} systems, rather than those seen in Fe^{IV} species. The predominant resonance structure is thus $Fe^{II}\leftarrow\{:C(X)Y\}^0$, quite different to the double-bond picture ($Fe^{IV}=\{C(X)Y\}^{2-}$, analogous to $Fe^{IV}=O^{2-}$) used in much current literature,[2a–c, 2f, 2h, 5a] but is consistent with earlier spectroscopic suggestions[5c, d] and their electrophilic reactivities.[2f, 2h, 5a, 7] The less favorable Fe^{IV} state in IPC complexes as compared to $Fe^{IV}=O^{2-}$ intermediates is, however, reasonable, since carbon has a lower electronegativity than oxygen.

The results described above are of broad general interest since they represent the first successful predictions of the Mössbauer spectra (δ_{Fe}, ΔE_Q), the ^{13}C NMR chemical shifts/shieldings as well as the local geometries of IPC complexes. They also provide the first theoretical basis for the origin of their electrophilic catalytic nature and also indicate that ^{13}C NMR spectroscopy may be a useful probe of IPC reactivity. Unlike the frequently used picture of a double bond between iron and carbon[2a-c, 2f, 2h, 5a] as being analogous to the catalytic intermediates in conventional P450 reactions ($Fe^{IV}=O^{2-}$), IPC complexes are

best described as involving $Fe^{II}\leftarrow\{:C(X)Y\}^0$, a result that should facilitate future studies of IPC systems in catalysis, and in bioinorganic chemistry.

Supplementary Material

Refer to Web version on PubMed Central for supplementary material.

References

1. a) Meunier B, de Visser SP, Shaik S. Chem Rev. 2004; 104:3947–3980. [PubMed: 15352783] b) Bernhardt R. J Biotech. 2006; 124:128–145.c) de Visser SP, Kumar D, Cohen S, Shacham R, Shaik S. J Am Chem Soc. 2004; 126:8362–8363. [PubMed: 15237977] d) Irigaray P, Belpomme D. Carcinogenesis. 2010; 31:135–148. [PubMed: 19858070]
2. a) Coehlo PS, Brustad EM, Kannan A, Arnold FH. Science. 2013; 339:307–310. [PubMed: 23258409] b) Che CM, Lo VKY, Zhou CY, Huang JS. Chem Soc Rev. 2011; 40:1950–1975. [PubMed: 21387046] c) Che CM, Zhou CY, Wong ELM. Top Organomet Chem. 2011; 33:111–138.d) Lu H, Dzik WI, Xu X, Wojtas L, de Bruin B, Zhang XP. J Am Chem Soc. 2011; 133:8518–8521. [PubMed: 21563829] e) Chan KS, Lau CM, Yeung SK, Lai TH. Organometallics. 2007; 26:1981–1985.f) Li Y, Huang JS, Zhou ZY, Che CM, You XZ. J Am Chem Soc. 2002; 124:13185–13193. [PubMed: 12405847] g) Thu HY, Tong GSM, Huang JS, Chan SLF, Deng QH, Che CM. Angew Chem-Int Edit. 2008; 47:9747–9751.h) Mbuvi HA, Woo LK. Organometallics. 2008; 27:637–645.i) Wang JC, Xu ZJ, Guo Z, Deng QH, Zhou CY, Wan XL, Che CM. Chem Comm. 2012; 48:4299–4301. [PubMed: 22447038] j) Li Y, Huang JS, Zhou ZY, Che CM. J Am Chem Soc. 2001; 123:4843–4844. [PubMed: 11457298] k) Chen Y, Huang LY, Zhang XP. Org Lett. 2003; 5:2493–2496. [PubMed: 12841763] l) Baumann LK, Mbuvi HM, Du G, Woo LK. Organometallics. 2007; 26:3995–4002.
3. Mansuy D, Lange M, Chottard JC, Guerin P, Morliere P, Brault D, Rougee M. J Chem Soc, Chem Comm. 1977:648–649.
4. a) Simonneaux G, Le Maux P. Top Organomet Chem. 2006:83–122.b) Tolando R, Ferrara R, Eldirdiri NI, Albores A, King LJ, Manno M. Xenobiotica. 1996; 26:425–435. [PubMed: 9173683] c) Mansuy D, Battioni JP, Chottard JC, Ullrich V. J Am Chem Soc. 1979; 101:3971–3973.d) Groves JT, Avaria-Neisser GE, Fish KM, Imachi M, Kuczkowski RL. J Am Chem Soc. 1986; 108:3837–3838.e) Lafite P, Dijols S, Zeldin DC, Dansette PM, Mansuy D. Arch Biochem Biophys. 2007; 464:155–168. [PubMed: 17470359] f) Taxak N, Patel B, Bharatam PV. Inorg Chem. 2013; 52:5097–5109. [PubMed: 23560646]
5. a) Lai TS, Chan FY, So PK, Ma DL, Wong KY, Che CM. Dalton Trans. 2006:4845–4851. [PubMed: 17033710] b) Mansuy D, Lange M, Chottard JC, Bartoli JF, Chevrier B, Weiss R. Angew Chem Int Ed. 1978; 17:781–782.c) Mansuy D, Battioni JP, Lavallee DK, Fischer J, Weiss R. Inorg Chem. 1988; 27:1052–1056.d) Guerin P, Battioni JP, Chottard JC, Mansuy D. J Organomet Chem. 1981; 218:201–209.e) English DR, Hendrickson DN, Suslick KS. Inorg Chem. 1983; 22:367–368.
6. Tatsumi T, Hoffmann R. Inorg Chem. 1981; 20:3771–3784.
7. Wolf JR, Hamaker CG, Djukic JP, Kodadek T, Woo LK. J Am Chem Soc. 1995; 117:9194–9199.
8. Rohde JU, In JH, Lim MH, Brennessel WW, Bukowski MR, Stubna A, Munck E, Nam W, Que L. Science. 2003; 299:1037–1039. [PubMed: 12586936]
9. a) Kachalova GS, Popov AN, Bartunik HD. Science. 1999; 284:473–476. [PubMed: 10205052] b) Debrunner, PG. Iron Porphyrins. Lever, ABP.; Gray, HB., editors. Vol. 3. VCH Publishers; New York: 1989. p. 139-234.
10. a) Ling Y, Zhang Y. J Am Chem Soc. 2009; 131:6386–6388. [PubMed: 19415933] b) Katigbak J, Zhang Y. J Phys Chem Lett. 2012; 3:3503–3508. [PubMed: 23205186] c) Zhang Y, Mao JH, Oldfield E. J Am Chem Soc. 2002; 124:7829–7839. [PubMed: 12083937] d) Zhang Y, Mao JH, Godbout N, Oldfield E. J Am Chem Soc. 2002; 124:13921–13930. [PubMed: 12431124]
11. Guillaume V, Thominot P, Coat F, Mari A, Lapinte C. J Organomet Chem. 1998; 565:75–80.
12. Ling Y, Davidson VL, Zhang Y. J Phys Chem Lett. 2010; 1:2936–2939. [PubMed: 20953337]

13. a) Andres H, Bominaar EL, Smith JM, Eckert NA, Holland PL, Munck E. J Am Chem Soc. 2002; 124:3012–3025. [PubMed: 11902893] b) MacDonnell FM, Ruhlandt-Senge K, Ellison JJ, Holm RH, Power PP. Inorg Chem. 1995; 34:1815–1822.c) Zhang Y, Oldfield E. J Phys Chem B. 2003; 107:7180–7188.
14. a) Costas M, Mehn MP, Jensen MP, Que L. Chem Rev. 2004; 104:939–986. [PubMed: 14871146] b) Ikezaki A, Ohgo Y, Nakamura M. Coord Chem Rev. 2009; 253:2056–2069.
15. Zhang Y, Oldfield E. J Am Chem Soc. 2004; 126:4470–4471. [PubMed: 15070336]

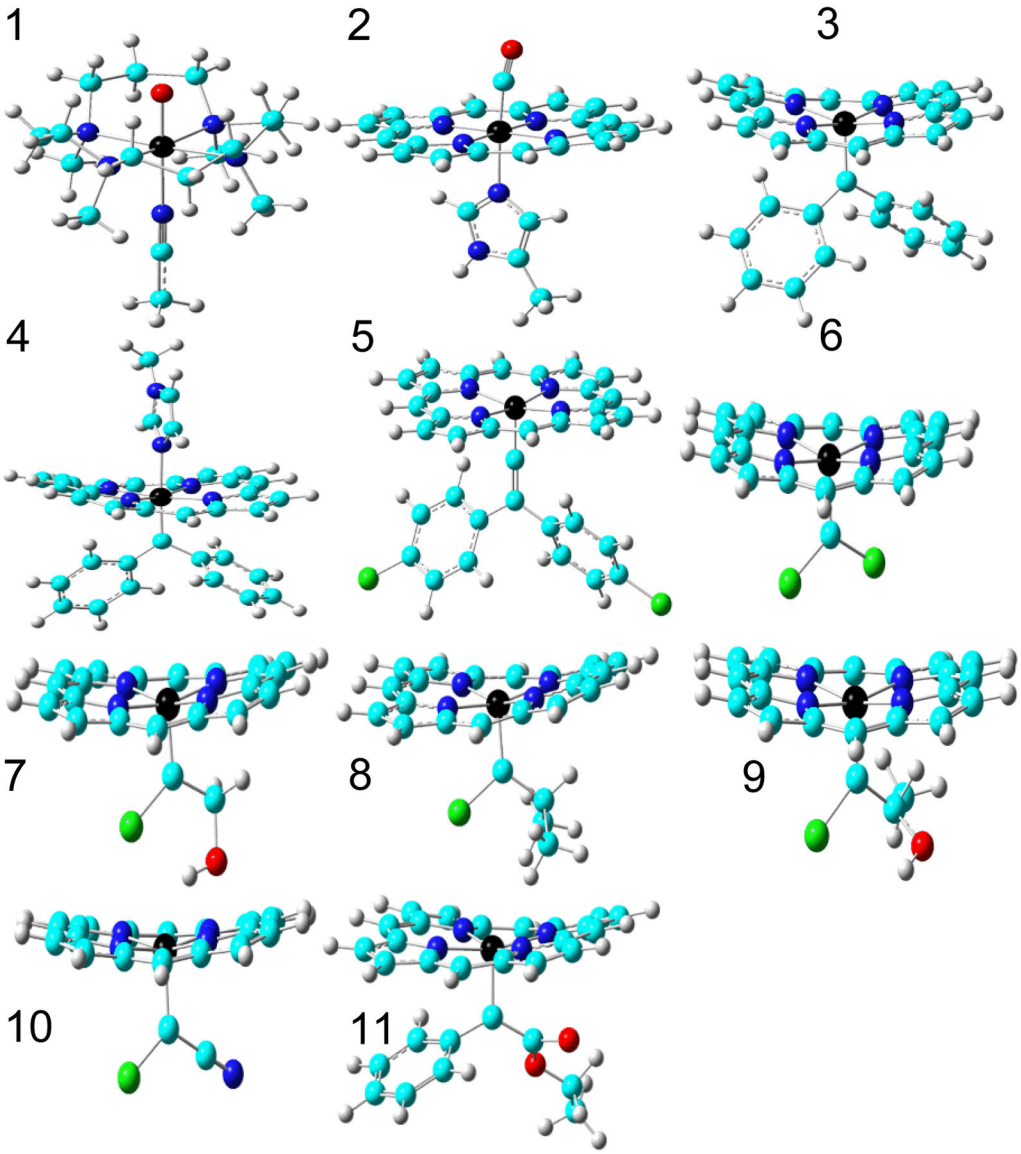

Figure 1.

Molecular models used in this work for **1** $[Fe^{IV}(O)(TMC)(NCCH_3)]^{2+}$, TMC = 1,4,8,11-tetramethyl-1,4,8,11-tetraazacyclotetradecane; **2** MbCO active site; **3** $[Fe(TPFPP)(CPh_2)]$, TPFPP = *meso*-tetrakis(penta-fluorophenyl)porphyrinato dianion; **4** $[Fe(TPFPP)(CPh_2)(MeIm)]$, MeIm = *N*-methylimidazole; **5** $[Fe(TPP)(C{=}C(C_6H_4Cl)_2)]$, TPP = *meso*-tetraphenylporphyrinato dianion; **6** $[Fe(TPP)(CCl_2)]$; **7** $[Fe(TPP)(CCl(CH_2OH))]$; **8** $[Fe(TPP)(CCl(CHMe_2))]$; **9** [Fe(TPP)(CCl(CHMe(OH))]; **10** [Fe(TPP)(CClCN)]; **11** $[Fe(TPFPP)(C(Ph)CO_2Et)]$. Atom colors: N - blue, O - red, C - cyan, H - grey, Fe - black, Cl - green.

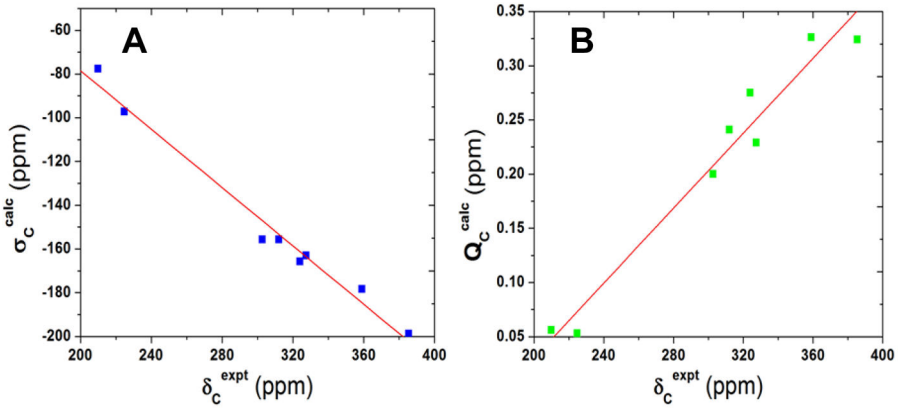

Figure 2.

Plots of (**A**) computed ^{13}C NMR chemical shieldings and (**B**) charges versus experimental ^{13}C NMR chemical shifts in IPCs.

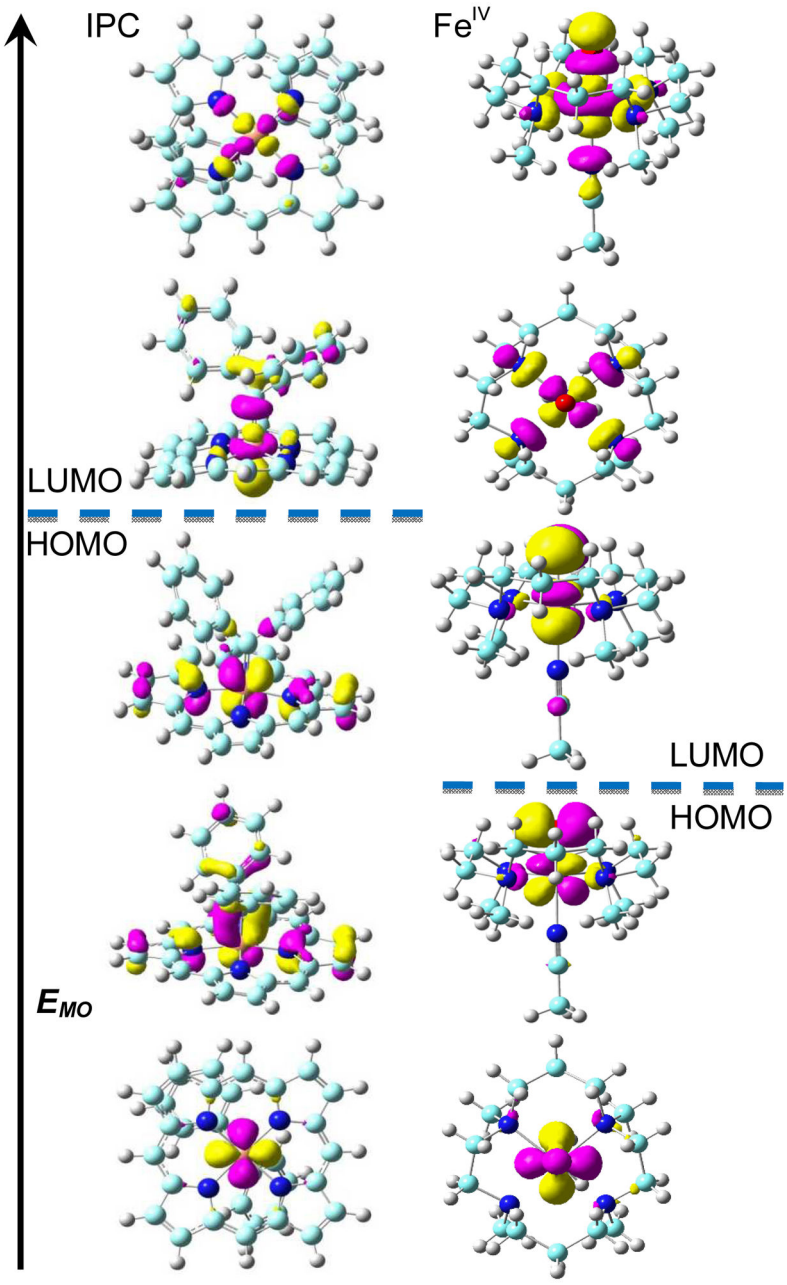

Figure 3.
Frontier metal MO diagrams of IPC complex **3** (left) and **1** (right) with S=0.

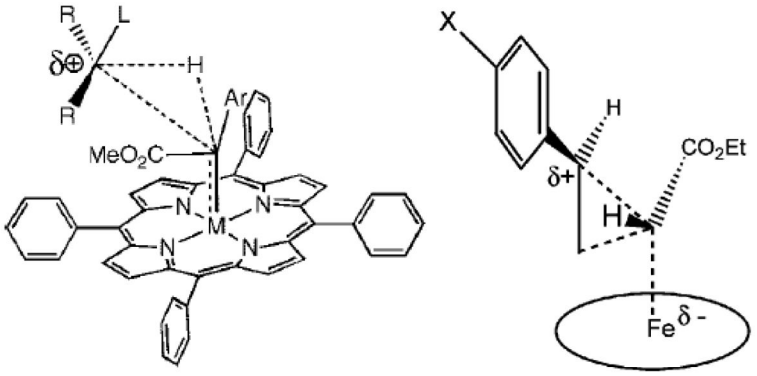

Scheme 1.

Experimentally proposed transition states in C-H insertion (left, Ref.2h) and cyclopropanation (right, Ref.5a) by IPCs.

Table 1

Mössbauer properties of Fe^{IV}, Fe^{II} and IPC complexes

System		S	δ_{Fe}(mm/s)	ΔE_Q(mm/s)	$\Delta E_{S=0}$(kcal/mol)
$[Fe^{IV}(O)(TMC)(NCCH_3)]^{2+}$	Expt[a)]	1	0.17	1.24	
1	Calc	0	0.11	−3.22	0.00
		1	0.13	1.25	−28.74
		2	0.097	0.53	−13.28
MbCO	Expt[b)]	0	0.27	0.35	
2	Calc	0	0.29	0.27	0.00
		1	0.38	0.33	30.99
		2	0.48	2.87	58.40
$[Fe(TPFPP)(CPh_2)]$	Expt[c)]	0	0.03	(−)2.34	
3	Calc	0	0.10	−2.37	0.00
		1	0.053	−2.97	20.61
		2	0.056	−2.90	69.16

[a)] Ref.8

[b)] Ref.9b

[c)] Ref.2f. The sign was not determined experimentally.

Table 2

X-ray and computed geometric properties of IPCs

System		S	R_{FeC}(Å)	R_{FeN}(Å)	R_{CC}(Å)
[Fe(TPFPP)(CPh_2)(MeIm)]	Expt[a)]	0	1.827	1.973	1.495
4	Calc	0	1.828	2.002	1.478
		1	2.018	1.993	1.458
		2	2.048	2.093	1.458
Fe(TFPP)($C(Ph)_2$)	Expt[a)]	0	1.767	1.967	1.483
3	Calc	0	1.764	1.991	1.478
		1	1.969	1.980	1.454
		2	2.030	2.112	1.453
[Fe(TPP)($C=C(C_6H_4Cl)_2$)]	Expt[b)]	0	1.690	1.985	1.487
5	Calc	0	1.675	1.992	1.484
		1	1.751	2.050	1.485
		2	2.058	2.000	1.489

[a)] Ref.2f

[b)] Ref.5c

Table 3

^{13}C NMR chemical shifts/shieldings and charges

	$\delta^{expt\ a)}$(ppm)	σ^{calc} (S=0)(ppm)	δ^{pred} (S=0)(ppm)	δ^{pred} (S=1)(ppm)	δ^{pred} (S=2)(ppm)	Q_C(e)
4	385.44	−198.88	380.27	2857.51	15809.38	0.324
3	358.98	−178.38	349.57	800.64	9408.93	0.326
11	327.47	−163.06	326.61	1075.39	12579.69	0.229
8	324.00	−165.80	330.73	22695.04	23522.84	0.275
9	312.00	−155.75	315.66	21584.70	21712.35	0.241
7	302.70	−155.77	315.69	21592.17	28689.45	0.200
6	224.70	−97.29	228.08	3421.81	74530.39	0.053
10	210.00	−77.57	198.53	1386.70	51894.04	0.056

*a)*Refs. 2c, 2f, and 5d.